Electrical Reliabilities of Highly Cross-Linked Porous Silica Film with Cesium Doping

Yasuhisa Kayaba,[1] Kazuo Kohmura,[2] Hirofumi Tanaka,[2] Yutaka Seino,[3] Toshiyuki Odaira,[4] Fumitaka Nishiyama,[5] Keizo Kinoshita,[6] Shinichi Chikaki,[6] and Takamaro Kikkawa[1]

[1]Research Institute of Integrated Science for Nanodevices and Bio Systems, Hiroshima University, Higashi-hiroshima, Hiroshima 739-8527, Japan.

[2]Product Development Laboratory, Mitsui Chemicals, Inc., 580-32, Nagaura, Sodegaura, Chiba 299-0265 Japan.

[3]Advanced Semiconductor Research Center, National Institute of Advanced Industrial Science and Technology (AIST), 16-1 Onogawa, Tsukuba, Ibaraki 305-8569, Japan.

[4]Research Institute of Instrumentation Frontier, National Institute of Advanced Industrial Science and Technology (AIST), 16-1 Onogawa, Tsukuba, Ibaraki 305-8568, Japan.

[5]Radiation Research Facility, Hiroshima University, Higashi-hiroshima 739-8527, Japan.

[6]Semiconductor Leading Edge Technologies, Inc. (SELETE), 16-1 Onogawa, Tsukuba, Ibaraki 305-8569, Japan.

A highly cross-linked porous silica dielectric (PoSiO) film was fabricated at a low temperature of 350°C. PoSiO films were derived by sol-gel method and their pore surface silanol groups were silylated with 1,3,5,7-tetramethylcyclotetrasiloxane (TMCTS) by vapor phase treatment. To promote the degree of siloxane cross-linkage of the film, cesium (Cs) was added to the precursor solution with the amount of 0, 5, 15, and 30 wt.-ppm as a catalyst. Then the amount of methyl-silicon-three oxygen (Me-Si T-type) and hydrogen-silicon-three oxygen (H-Si T-type) bridged structures of the chemisorbed TMCTS were increased, and the amount of surface silanol groups was decreased markedly with the increasing amount of Cs concentration. Leakage current and dielectric constant were measured under various humidity conditions, and which were hardly degraded for the highly cross-linked PoSiO owing to its small amount of residual silanol groups

and adsorbed water. It was also shown that the amount of mobile protons originated from the silanol groups became negligible. Time zero dielectric breakdown (TZDB) field strength was improved to 6.7 MV/cm and a projected time dependent dielectric breakdown (TDDB) lifetime satisfied 10 years for Cs 30 ppm doped PoSiO under a stress conditions of 220°C and $/E/ = 1$ MV/cm.

I. INTRODUCTION

For the sake of the resistance-capacitance signal delay time reduction and the power consumption in large-scale integrated circuits (LSI), highly reliable low dielectric constant (low-k) insulator films must be fabricated. Sol-gel derived porous silica film (PoSiO), which has a rigid silica skeleton, air pores having diameters of a few nm, and ultra low dielectric constant under 2.3,[1,2] is a promising candidate for it. It needs to be fabricated it at a low temperature of 350°C to maintain the reliability of cupper (Cu) interconnect, but then the degree of cross-linkage of PoSiO becomes insufficient and we need to struggle to satisfy the high electrical reliabilities, as discussed in this section. PoSiO fabricated at a low temperature has a large amount of silanol groups on its large pore surface area, and the silanol groups adsorb water in humid vapor. Then its dielectric constant markedly increases proportional to the amount of adsorbed water because the dielectric constant of water is approximately 80.[3,4] Next we'll consider the degradation mechanism of leakage current. Unlike the case of thin thermal oxide, direct tunneling current is negligible here. Schottky current or Fowler-Nordheim tunneling current should not appear at electric field strength of few MV/cm, because amorphous silica skeleton has enough high conduction band level compared to Fermi level of metal electrode and large band gap. Then a serious problem is proton conducting leakage current originated from residual silanol groups.[5-7] This ionic leakage current increases in proportion to the amount of silanol groups and adsorbed water, and which exists at almost zero electric field strength.[5,6] Therefore, reduction of the amount of silanol groups and water adsorption are the most serious issues for the insurance of reliability. To avoid the above degradations, the silanol group must be eliminated by promoting the siloxane cross linkage between

next neighboring silanol groups or replacing it with hydrophobic group such as methyl-silicon, hydrogen-silicon by using silylation agents e.g. hexamethyldisilazane (HMDS), 1,3,5,7-tetramethylcyclotetrasiloxane (TMCTS),.. etc. Here, we'll discuss about dielectric strength. For the case of thin thermal oxide, its mechanism is well studied and many models are proposed for time dependent dielectric breakdown (TDDB) lifetime, for example, field acceleration models such as E model[8,9] and $1/E$ model[10]. In contrast to this, for the case of porous silica films the mechanism of TDDB become more complex because of its internal electric field fluctuation.[11] However, primary degradation of TDDB lifetime must be initiated at the weak chemical bonds such as silanol group (SiOH). Porous silica films have large amount of such weak bonds, if they are fabricated at low temperature. These must be changed to more strong bonds in order to satisfy 10-years TDDB lifetime under a high stress conditions.

Fujii *et al.* studied about a porous silica film with TMCTS treatment, and they reported that the cesium (Cs) catalyst promoted the degree of siloxane cross linkage and high mechanical strength was obtained.[12] In this paper, we report the Cs doping effect on the electrical reliabilities of PoSiO film that is fabricated at a low temperature of 350°C. After seeing chemical bonding structures, humidity effect on dielectric constant is measured and water adsorption isotherm is calculated from the dielectric constant. Leakage current properties are measured under humid vapor and nitrogen vapor. Possible mobile ions such as H^+, Cs^+ are searched by using triangular voltage sweep (TVS) technique. Time zero dielectric breakdown (TZDB) field strength is measured and its statistical properties are discussed. Then time dependent dielectric breakdown lifetimes

under several stress conditions are measured.

II. EXPERIMENT

A precursor solution of porous silica was synthesized from an acidic silica sol derived from tetraethylorthosilicate (TEOS) in ethanol diluted with water and a nonionic surfactant polyoxyethylene-20-stearylether (Brij-78).[13] In order to increase the degree of siloxane cross-linkage of the resulting PoSiO, small amount of cesium nitrate ($CsNO_3$) was added to the precursor solution. The doped concentrations of Cs were 0, 5, 15, and 30 wt.-ppm. Each solution was spin-coated on a 300-mm diameter silicon (Si) wafer and cured under nitrogen (N_2) ambient at 150°C. After being annealed at 350°C in TMCTS vapor for 90 min., the surfactant was removed with the aid of ultra-violet (UV) irradiation with heated Si substrate at 350°C, and a few nm scale air pores were formed in the silica skeleton. The resulting films were baked at 350°C in TMCTS vapor for 90 min. The wafers were cut into 3.5 cm x 3.5 cm dies to measure the film properties. Film thickness and refractive index were measured by spectroscopic ellipsometer in humid vapor at room temperature. Chemical bonding structures were measured by transmission Fourier transform infra-red spectroscopy (FT-IR) under N_2 vapor. Here, the incident beam angle was taken at the Brewster angle of silicon (Si) substrate to enhance the signal intensity. Atomic ratio of oxygen (O) or Cs to Si were determined from Rutherford backscattering spectrometry (RBS). Accelerated He ion with a kinetic energy of 2 MeV was passed through the silicon substrate at the channeling angle of it, and the scattered ion was detected at a backward angle of 100 degree relative to the incidental beam

angle. The mechanical strength of PoSiO films was measured by nono indentater with a Berkovitch pyramidal indentations tip. The depth of indentation was taken within 10 to 30 nm for 140 to 170-nm thick PoSiO films.

To evaluate the electrical properties of PoSiO, 2-mm diameter circle electrodes were formed on the top of the samples using vacuum vapor deposition. Here the metal was gold (Au) for the measurements under humid vapor in order to avoid degradation of electrode, and aluminum (Al) for the measurements under nitrogen (N_2) vapor, respectively. The metal/PoSiO/Si capacitors were put into the N_2 purged globe box (relative humidity condition (RH) of 2%), and being baked at 200°C for 10 hours to desorb physically adsorbed water. Then C-V or I-V characteristics were measured under various RH range from 2% to 65%. Here, RH was controlled by introducing humid vapor with regulating N_2 flow to the box. These measurements were performed after water adsorption reached to equilibrium. Sampling frequency of capacitance was 100 kHz and tan δ was always in the order of 10^{-2}. To determine the dielectric constant of PoSiO film from capacitance in high precision, pad area of Au electrode was measured by optical microscope.

TVS measurement was carried out under N_2 ambient and Si substrate was heated at 200°C. After a constant electric field strength (E_c) of −1 MV/cm was applied to the gate metal for a few minuets to accumulate positively charged mobile ions to metal/PoSiO interface, leakage current density (J) was measured with sweeping the electric field strength from $-|E_c|$ to $|E_c|$ with a ramp rate ($\beta = dE/dt$). In the same way, after a constant stress of E_c = +1 MV/cm was applied, J-E characteristic was also measured. TZDB electric field strength was measured under nitrogen

vapor with heated Si substrate at 200°C. In the TDDB lifetime measurement, 16 capacitors were sampled together by using a probe card. The 16 probes were connected to a source meter via switching matrix unit, and a constant bias stress was always applied to the 16 capacitors. After each probe was switched to a semiconductor parameter analyzer via switching matrix unit one by one, leakage current was measured with the same constant bias voltage then detected whether the capacitor was destructed or not. Above measurements were performed semi-automatically with LabVIEW programs.

III. RESULTS AND DISCUSSION

A. Film Properties

Figure 1 represents each atomic ratio of Cs/Si and O/Si as a function of doped Cs density. The relationship between Cs/Si and doped Cs density was approximately linear and Cs 30 ppm PoSiO had 0.035%. The O/Si ratio was decreased at first then became large with the increasing amount of doped Cs density. With the results of chemical bonding composition represented below, it is assumed that the first decrease was due to the decrease of silanol groups. The following increase of O/Si ratio was due to the increase of siloxane cross linkage of silica skeleton, and the co-polymerization of TMCTS molecules via H-Si or Me-Si T-type bridged structures. Film thickness (d) and refractive index (n) are compiled in Table 1. The film thickness shrunk and refractive index was increased as doped Cs concentration increased. The porosity (P) was determined from the k at RH 0% by using Rayleigh equation (eq. (1)) for PoSiO which has cylindrical pore and silica skeleton,

$$P = \frac{k_{silica}^{2} - kk_{silica} - k + k_{silica}}{k_{silica}^{2} + k_{silica}k - k - k_{silica}}, \qquad (1)$$

where k_{silica} (= 3.9) is the dielectric constant of silica skeleton. The dielectric constants of Cs doped

PoSiO with 0, 5, 15, and 30 ppm were 1.89, 1.92, 1.98, and 2.06, respectively. Here the k at RH 0%

was obtained by extrapolating the k-R_h relation shown in Fig. 6. Then the porosities were

obtained as 0.587, 0.576, 0.545, and 0.521, respectively. Figure 2 shows the elastic modulus as a

function of porosity. From a finite element analysis the elastic modulus (M) is described by

$$M = M_w(1 - P)^2, \qquad (2)$$

here, M_w is the elastic modulus of silica skeleton.[14] By comparing this equation with the experimental

results, M_w were obtained as 10, 17, 31, 31 GPa for Cs 0, 5, 15, 30 ppm PoSiO, respectively. Therefore,

the enhancement of mechanical strength owing to Cs doping was also occurred even for the PoSiO,

which was fabricated at a low temperature of 350°C, as reported in the case of PoSiO fabricated at

400°C.[12] Figure 3 shows pore size distribution measured from positron annihilation lifetime

spectroscopy (PALS). The mean pore size of Cs 0 ppm doped PoSiO was 3.53 nm. By increasing doped

Cs concentration the amount of large pore was decreased and the mean pore diameter decreased as

3.34, 3.21, and 2.95 nm, respectively. A possible reason of this decrease is owing to additional

adsorption of TMCTS molecule on pore surface. According to ref. 15 the thickness of monolayer

TMCTS fabricated on flat oxide surface is 0.49 nm so the thickness of additional TMCTS shell was

approximately the half of monolayer of TMCTS. If the pore surface of Cs 0 ppm PoSiO was filled with

monolayer TMCTS then the pore diameter without silylation was 4.51 nm. With the porosity and the

mean pore size (a) the pore surface area (S) per unit volume (V_0) could be estimated by using an

equation of $S/V_0 = \pi\ a/V_0 = \pi\ a/(\pi\ (a/2)^2)\ P = 4\ P/a$ for cylindrical air pore. Then we have the pore

surface area as 0.665, 0.690, 0.679, 0.706 nm^2 per unit volume of nm^3 for Cs doped PoSiO with 0, 5,

15, and 30 wt.-ppm, respectively.

B. Chemical Bonding Structure

In Fig. 4 the FT-IR spectra of PoSiO films are shown, where adsorption intensity is

normalized to the film thickness and the pore surface area. In Fig. 4(b) the FTIR spectra at low

wave numbers range from 800 to 1400 cm^{-1} are shown. Broad and intense peaks at 1000-1250

cm^{-1} correspond to asymmetric vibration mode of network Si-O-Si bond. In Cs doped sample the

area of Si-O-Si peak increased compared to that of non-doped sample and differential spectra

between Cs doped and non-doped sample had broad peaks centered at 1190 cm^{-1} and 1060 cm^{-1}.

The peak at 1060 cm^{-1} is due to a ladder-like siloxane network. These increased amounts of

siloxane network should originate from additional adsorption of TMCTS, and co-polymerization

between next-neighboring TMCTS, and siloxane cross-linkage of silica skeleton. With this data

we could not split out the two contributions. A peak at 1265 cm^{-1} is C-H stretching mode of

$H(CH_3)SiO_2$ (D-type) structure,[16,17] which is non-bridged moiety of chemisorbed TMCTS. Its peak

intensity was decreased with the increasing Cs concentration. On the other hand, a peak at 1280

cm^{-1} is C-H stretching mode of $(CH_3)SiO_3$ (Si-Me T-type) structure,[16,17] which is bridged structure

between TMCTS and pore surface silica or next neighboring TMCTS. The peak intensity was

increased as 0.08, 0.18, 0.29, and 0.29 for Cs 0, 5, 15, and 30 wt.-ppm PoSiO. Therefore, the degree

of siloxane cross-linkage of TMCTS via Si-Me T-type structure was promoted by Cs doping. The two peaks due to each C-H stretching mode overlap with the broad peak of Si-O-Si vibration mode, and it is difficult to split out each element.

The FT-IR spectra with higher wave numbers ranging from 2000 to 4000 cm^{-1} are shown in Fig. 4(a). A peak at 3740 cm^{-1} corresponds to O-H stretching mode of isolated silanol group and a broad peak between 3200 and 3720 cm^{-1} corresponds to the same mode of hydrogen bonded silanol group. Figure 5(a) shows the peak area of each O-H stretching mode. The total area means the sum of the above two areas. All of them were monotonically decreased as Cs concentration increased. The amount of total OH for Cs 30 wt.-ppm doped PoSiO was 1/5 of non-doped PoSiO. The peak at 2970 cm^{-1} of Fig. 4(a) is C-H stretching mode of methyl (CH$_3$) group of TMCTS. The peak at 2920 cm^{-1} and the shoulder at 2880 cm^{-1} is the same mode of CH$_2$ group. Figure 5(b) shows the peak area of methyl group. The area was increased as doped Cs concentration increased and so the amount of chemisorbed TMCTS molecule was increased. The amount of methyl group for Cs 30 wt.-ppm doped PoSiO was 1.6 times larger than that of non-doped PoSiO. In Fig. 4(a) there are two peaks around 2200 cm^{-1} due to H-Si stretching mode of TMCTS. The peak at 2180 cm^{-1} corresponds to Si-H stretching modes of D-type structure[18,19] of TMCTS. Figure 5(c) shows these peak areas. The amount of D-type structure was decreased for doped PoSiO with Cs 0, 5, and 15 wt.-ppm, and saturated for doped PoSiO with Cs 30 wt.-ppm. Figure 5(d) shows the peak area ratio of D-type structure relative to that of CH$_3$. From this result the degree of siloxane cross-linkage of TMCTS is estimated as follows. When TMCTS molecules are chemisorbed on pore surface via dehydrogenation process, then the ratio of D-type/CH$_3$ remains

constant independent of the number of adsorbed TMCTS. However, the area ratio of D-type/CH$_3$ was decreased as Cs concentration increased and the area ratio for Cs 30 wt.-ppm doped PoSiO became 1/4 of non-doped PoSiO. The decreased amount corresponds to the increased amount of Me-Si T type structure of TMCTS. In addition to above results, the Si-H stretching mode of H-Si-O$_3$ (H-Si T-type) structure of TMCTS was found between 2250 and 2280 cm^{-1}.[12,18-25] As shown in Fig. 5(c), the peak area was increased with increasing Cs concentration up to 15 wt.-ppm, and decreased slightly for Cs 30 wt.-ppm. When we compare the peak area to that of D-type structure then the area ratio increased with the increasing Cs concentration up to 15 wt.-ppm and decreased slightly for Cs 30 wt.-ppm as seen in Fig. 5(d). The area ratio of H-Si T-type/D-type with Cs 30 wt.-ppm was 10 times larger than that of non-doped PoSiO. As a result, Cs doping promoted not only Me-Si T-type structure but also H-Si T-type bridged structure of TMCTS.

C. Water Adsorption Property

FTIR spectra show the decrease of silanol groups for Cs doped PoSiO. However, we have to measure the influence of humidity on dielectric constant and water adsorption property of the PoSiO, because we don't know if these silanol groups exist in silica skeleton or on pore surface. Another interest is to measure absolute amount of water adsorption site. By the use of a method represented in ref. 4, the Brunauer-Emmett-Teller (BET) adsorption area of water could be obtained from capacitance of ordinary metal-insulator-silicon (MIS) or metal-insulator-metal (MIM) structure without destructing the insulator film.

Figure 6 shows the dielectric constants calculated from the capacitance values at each relative humidity condition (R_h). By extrapolating the experimental data to RH 0% with a linear function of R_h, the dielectric constants for Cs 0, 5, 15, and 30 ppm PoSiO at RH 0% were determined as 1.89, 1.92, 1.98, and 2.06, respectively. When we calculate the increased amount of the dielectric constant relative to that of RH 0%, the influence of humidity on it is decreased by Cs doping. For example, at RH 65% the increased amount of non-doped PoSiO was 39% but that of doped PoSiO with Cs 30 wt.-ppm was only 4%. Figure 7(a) is a water adsorption isotherm at room temperature. Vertical axis is the number density of adsorbed water per unit pore surface area (N), which was calculated from dielectric constant by using a modified Rayleigh equation and Kirkwood theory.[3] In our calculation Kirkwood z parameter was set equal to 0, because water cluster formation is suppressed on hydrophobic surface.[4] In addition to this, we assumed a volume fraction of adsorbed water shell to the pore (v_{shell}) as 0.1. Then N was decreased markedly with the increasing Cs concentration. To obtain the number density of water adsorption site (N_m) and adsorption energy ($E_0 - E_L$), a BET plot of the water adsorption isotherm was taken as shown in Fig. 7(b). The data that behaved in linear were fitted by BET equation of

$$\frac{R_h}{N(1 - R_h)} = \frac{1}{N_m c}\left(1 + (c - 1)R_h\right), \tag{3}$$

here $c = exp((E_0 - E_L)/k_B T)$ is a BET parameter. The fitting range was taken around RH 20-40% and resulting N_m is depicted in Fig. 8(a). $E_0 - E_L$ are 0.066, 0.069, 0.040, and 0.054 eV for doped PoSiO with Cs 0, 5, 15, and 30 ppm, respectively. To estimate an error due to v_{shell}, the another result with $v_{shell} = 0.01$ was also calculated and shown in Fig. 8(a). The difference between the N_m

with $v_{shell} = 0.1$ and that with $v_{shell} = 0.01$ was 17% and $E_0 - E_L$ was 9%. With increasing doped Cs concentration N_m was decreased monotonically but there was no correlation between $E_0 - E_L$ and Cs concentration. N_m of non-doped PoSiO was 1.312 /nm² but that of doped PoSiO with Cs 30 wt.-ppm was 0.126 /nm². Figure 8(b) is a relationship between the total area of O-H stretching mode from FT-IR spectra (S_{OH}) and N_m. The relationship was described well by a simple linear function of $S_{OH} = A + B\,N_m$ with $A = -0.1057 \pm 0.068$ and $B = 0.772 \pm 0.066$, where the errors mean a fitting error. A was consistent with 0 within $2\,\sigma$ error. Therefore, the decreased amount of S_{OH} approximately represents the decreased amount of surface silanol groups that adsorbed water.

D. Leakage Current Properties

Figure 9(a) is leakage current density under a constant bias stress of -1 MV/cm as a function of elapsed time. The leakage current was decreased monotonically with elapsed time. This is due to the conduction of the finite number of mobile protons included in PoSiO. When the substrate temperature was 20°C, there was no difference among the samples. This result means the number of protons was the same for all samples. On the other hand, when the substrate was heated at 200°C, the leakage currents became larger. These currents were also decreased as a function of elapsed time; therefore, they are thermally activated proton conducting currents. The leakage current became smaller for the highly doped Cs PoSiO, because the amount of silanol group was smaller for larger Cs concentration. Figure 9(b) is a relationship between leakage current density with $E = -1$ MV/cm and elapsed time at 20°C under humid vapor of RH 59%. Before this measurement the samples were left at humid vapor for a few days to absorb water. In

contrast to the results under N_2 vapor, the leakage currents became steady. This is because the adsorbed water provides proton continuously. However, leakage current of Cs 0 ppm PoSiO reached to a compliance value soon after bias voltage was applied. The magnitude of leakage current was decreased markedly with the increasing Cs concentration. According to Nogami *et al.* the decrease must be due to the decreased amount of silanol group and adsorbed water.[5,6]

In Fig. 10, *E-J* characteristics at every RH 10% from RH 2% to 60% are shown. As described above, the *E-J* characteristic at RH 2% (under N_2 vapor) corresponds to a relaxation current of proton conduction, and which did not differ among all samples. Above the RH condition, leakage current began to increase and another *E-J* characteristic appeared for Cs 0, 5, 15 ppm PoSiO. The appeared *E-J* characteristic, which was saturated at high electric field strength over approximately 0.5 MV/cm, is resistive current of proton conducting. It is remarkable that the *E-J* characteristic of Cs 30 ppm PoSiO was not changed. A possible reason is that the proton-conducting path through adsorbed water was hardly formed due to the dense and highly cross-linked TMCTS on the pore surface.

E. Mobile Ion Detection

We discuss about mobile ion detection with the use of TVS measurement. TVS technique[26] is a very useful technique to investigate the existence and the kinetics of mobile ions. This technique is known to be applicable to metal/insulator/metal structure such as Cu/low-*k*/Cu interconnect, and it can distinguish ionic species such as proton, Cu^+, Na^+, and can determine its total electrical charge.[27-29]

Figure 11 (a) shows E-J characteristics of Cs 0 ppm PoSiO under N_2 ambient at 200°C after a constant bias stress of $/E_c/$ = 1 MV/cm was applied for 60 sec. A peak due to coherent motion of ion was measured, but that appeared only at the sweep from E_c = +1 MV/cm to −1 MV/cm. This asymmetric E-J characteristic was different from that of mobile alkali metal ions, in those cases, symmetric peaks appear.[30,31] We have to consider a possibility of metal ion injection from electrode within minus constant bias was stressed. However, it was not occurred because the same E-J characteristics were obtained when reversing the order of TVS measurement. Similar asymmetric results were obtained by Lifshitz et al,[30,31] they studied about the mobile charge in Al/porous spin-on oxide (SOX)/Si capacitor. They concluded that the mobile ion in SOX is proton and the free proton is accumulated only at the SOX/Si interface, then an asymmetric I-V characteristic is obtained. According to Hellins model the mobility μ of ion in metal/insulator/Si capacitor is described by

$$\mu = \frac{2d^2\beta}{(V_{peak} - \Phi_{MSi})^2} \, , \tag{4}$$

here d means insulator film thickness, V_{peak} is position of the peak, and Φ_{MSi} is metal-Si work function difference. In Fig. 11(a), the V_{peak} shifted to lower value with the decreased ramp rate, from these results the proton mobility was obtained as 3×10^{-12} cm²/(V·sec). With this mobility, the thermally activated proton conducts from Si/PoSiO interface to PoSiO/Al interface in 5-6 seconds with $E = -1$ MV/cm at 200°C. Then it is also revealed from Fig. 9(a) that, proton emission continued for a few minuets even under nitrogen ambient. On the other hand, in Fig. 11(b), we could not find a peak due to the proton motion in Cs 5, 15, 30 ppm PoSiO. However, background

currents were observed for all PoSiO. The background current means the monotonically increased current with increased bias voltage, and which may be originated from discharge of proton at Si/PoSiO or Al/PoSiO interface. This background current decreased with increasing Cs concentration, and which became less 10^{-9} A/cm^2 for Cs 15, 30 ppm PoSiO. As a result, it is revealed that Cs doping decreased the amount of proton and suppressed the proton conducting leakage current.

In addition to above discussions, we have to consider about the ionized charge density and the mobility of Cs in PoSiO. By using the atomic ratio of Cs/Si from RBS and film porosity the number density of Cs in Cs 30 ppm PoSiO, was obtained as 3.7×10^{14} /cm^2. The sensitivity of TVS measurement is 10^9 ion/cm^2, therefore this sensitivity is enough to detect ionized Cs unless its ionization rate is too low. To detect it other I-V measurements were performed until dielectric breakdown was occurred, but a peak due to mobile Cs ion was never detected. Here, the ramp rate was 1 V/sec and a constant bias of $|E_c|$ = 1 MV/cm was applied for 300 sec at 200°C before the measurements. Consequently, its mobility was lower than 8×10^{-14} cm^2/(V・sec). This very small mobility must be due to its large ionic radius of 169 pm as also reported in ref. 32.

F. Time Zero Dielectric Field Strength

A useful technique to investigate the dielectric strength is the statistical analysis of time zero dielectric breakdown (TZDB) field strength, which was first developed by Fritzshe.[33] In contrast to TDDB lifetime measurement, this measurement requires a shorter time so we could easily observe the effects of process condition and chemical compositions. These statistics help us to

understand the mechanism of dielectric breakdown.

Figure 12 shows E-J characteristics of PoSiO films at 200°C under N_2 ambient. In this measurement a minus bias stress was applied to Al electrode with the ramp rate of 1 V/sec until the leakage current reached to a compliance value of 10^{-6} A. There were three types of dielectric breakdown (DB) mode. First DB mode was the initial failure mode. In this mode the leakage current reached the compliance value at few volts. The reason of this breakdown may be due to a formation of leak path caused by mechanical breakdown of the film or pore aggregation that looks like pinhole. Second DB mode was instantaneous breakdown mode. Above finite electric field strength, leakage current was increased gradually or suddenly and reached to the compliance value, but the capacitor was still operational after they occurred. After repeating the same measurement, the capacitor resulted in permanent breakdown. Third DB mode was the permanent dielectric breakdown mode. Above high electric field strength over 3 MV/cm, the leakage current was increased suddenly and the capacitor were destructed. In Fig. 12 the solid line represents the E-J property due to the third DB mode and the dashed line is the second DB mode. For Cs 0 and 5 ppm PoSiO a few events of the second DB mode were observed at low electric field strength, however, for Cs 15 and 30 ppm PoSiO there were no differences between the E-J property of second and third DB mode. Figure 13 is a Weibull distribution of the TZDB field strength (E_{DB}). In Cs 0 and 5 ppm PoSiO the probability density of first DB mode were 30% and 20%, respectively. However, Cs 15 ppm PoSiO and Cs 30 ppm PoSiO did not have the first DB mode. So, 15 or 30 ppm Cs doping improved the yield ratio of PoSiO. On the other hand, the

distribution was significantly improved by Cs doping and its value of 50% probability were –3.4 MV/cm, –4.7 MV/cm, –6.2 MV/cm, and –6.7 MV/cm for Cs 0, 5, 15, and 30 ppm PoSiO, respectively.

To investigate the mechanism of dielectric breakdown of composite dielectrics we must consider the electrical field fluctuation in it, because dielectric breakdown is related to the maximum magnitude of the fluctuated electric field strength.[34] For the case of porous silica dielectric the maximum field strength (E_{max}) was studied by Kayaba and Kikkawa.[11] According to their work, E_{max} always appears at air/silica interface. If the pore surface is coated by TMCTS, the E_{max} hardly changes at the same porosity. Therefore, a possible reason of the enhancement of E_{DB} due to Cs doping is that the replacement of electrically weak bonds such as SiOH and unstable siloxane bond with strong bonds such as Si-C or stable siloxane bond, so electrical defects may be almost eliminated by Cs doping.

G. Time Dependent Dielectric Breakdown Lifetime

At last we discuss about the TDDB lifetime (t_{DB}) under N_2 ambient. It is reasonable to start with the E model, which merely describes that dielectric breakdown occurs in thermodynamic way as represented by

$$t_{DB} = A\exp\left(\frac{\Delta H_0}{k_B T}\right)\exp[\gamma(T)(E_{DB} - E)], \tag{5}$$

here t_{DB} is TDDB lifetime, A is a constant, ΔH_0 is change in enthalpy, k_B is Boltzmann constant, T is temperature, $\gamma(T)$ is a function of temperature, E_{DB} is time zero dielectric breakdown field

strength, and E is the applied field strength. It is remarkable that improvement of E_{DB} is important as the same as the improvement of ΔH_0 to enhance the TDDB lifetime. Figure 14(a) plots the t_{DB} of 50% probability ($t_{DB}(50\%)$) at 200°C of each PoSiO. For Cs 0 ppm PoSiO and Cs 5 ppm PoSiO the bias stress was –3 MV/cm and for Cs 15 and 30 ppm PoSiO it was changed within –4 and –5.5 MV/cm. In this figure the results obtained by TZDB measurement were also plotted. For the case of Cs 15 ppm PoSiO and Cs 30 ppm PoSiO the data was fitted by eq. (5) and extrapolated to $E = -3$ MV/ cm. Then it was found that $t_{DB}(50\%)$ was improved from 10^3 sec to 10^6 sec by Cs doping. On the other hand the results of Cs 15 ppm PoSiO and Cs 30 ppm PoSiO were consistent with the error of extrapolation. According to the E model this improvement is owing to the enhancement of E_{DB} as shown in Fig. 14(a). Figure 14(b) is the t_{DB} (50%) of Cs 30 ppm PoSiO with several stress conditions of 180°C, 200°C, 220°C, and bias stress within 4 - 6.5 MV/cm. Each data set was fitted well with eq. (5) and extrapolated to low electric field strength. Then the projected TDDB lifetime satisfied 10 years even at 220°C with $/E/ = 1$ MV/cm stress condition. Here the projected TDDB lifetime was underestimated by the amount of 1 σ extrapolation error.

IV. CONCLUSIONS

A highly cross-linked porous silica film silylated with 1,3,5,7-tetramethylcyclotetrasiloxane (TMCTS) was fabricated at low temperature of 350˚C. To promote the degree of siloxane linkage of the porous silica, cesium (Cs) was added to its precursor solution with the concentration of 0, 5, 15, and 30 wt.-ppm. Then the amount of methyl-silicon-three oxygen (Me-Si T-type) and hydrogen-silicon-three oxygen (H-Si T-type) bridged structures of TMCTS were increased, and silanol group was decreased markedly. Then electrical reliabilities were measured and high reliabilities were obtained for Cs 30 ppm doped porous silica. The influence of humidity on the increase of dielectric constant was suppressed to only 4% even at the relative humidity condition (RH) of 65% compared to that of RH 0%. The number density of water adsorption site (N_m) was derived from the dielectric constant and it was decreased from 1.312 to 0.126 /nm². Furthermore, the humidity effect on the leakage current became negligible. A triangular voltage sweep measurement under nitrogen ambient revealed the decrease of proton, and Cs ion was never detected even for Cs 30 ppm porous silica. Time zero dielectric breakdown field strength (E_{DB}) was improved from 3.4 MV/cm to 6.7 MV/cm. Owing to this improvement the TDDB lifetime was prolonged for Cs 30 ppm porous silica and its projected 10 year lifetime was satisfied under the stress conditions of 220°C and $|E| = 1$ MV/cm.

ACKNOWLEDGEMENTS

Tables

Table 1. Film thickness (d) and refractive index (n) from spectroscopic ellipsometry.

Cs density (wt.-ppm)	d (nm)	n
0	171.0	1.157
5	157.6	1.189
15	140.9	1.236
30	138.7	1.247

References

[1]K. Maex, M. R. Baklanov, D Shamiryan, F. lacopi, S. H. Brongersma, and Z. S. Yanovitskaya, J. Appl. Phys. **93**, 8793 (2003), and references therein.

[2]T. Kikkawa, S. Chikaki, R. Yagi, M. Shimoyama, Y. Shishida, N. Fujii, K. Kohmura, H. Tanaka, T. Nakayama, S. Hishiya, T. Ono, T. Yamanishi, A. Ishikawa, H. Matsuo, Y. Seino, N. Hata, T. Yoshino, S. Takada, J. Kawahara, and K. Kinoshita, Tech. Dig. IEEE Int. Electro. Dev. Meet., 99, (2005).

[3]T. Kikkawa, S. Kuroki, S. Sakamoto, K. Kohmura, H. Tanaka, and N. Hata: J. Electrochm. Soc., **152**, G560 (2005).

[4]S.-I. Kuroki and T. Kikkawa, J. Electrochem. Soc. **153**, G759 (2006).

[5]M. Nogami and Y. Abe, Phys. Rev. B **55**. 12 108 (1997).

[6]M. Nogami, R. Nagao and C. Wong, J. Phys. Chem. B **102**, 5772 (1998).

[7]Y. Kayaba, K. Kohmura, and T. Kikkawa, Extended Abstracts of SSDM (Japan Society of Applied

Phys., Yokohama), 1018 (2006).

[8]J. W. McPherson and D. A. Baglee, *International Reliability Physics Proceedings* (IEEE, Piscataway, NJ, 1979), 8.

[9]J. W. McPherson and D. A. Baglee, J. Electrochem. Soc. **132**, 1903 (1985).

[10]J. C. Lee, I. C. Chen, and C. Hu, IEEE Trans. Electron Devices **35**, 2268 (1988).

[11]Y. Kayaba and T. Kikkawa, Jpn. J. Appl. Phys. **47**, 5314 (2008).

[12]N. Fujii, K. Kohmura, T. Nakayama, H. Tanaka, N. Hata, Y. Seino, and T. Kikkawa, Proc. SPIE, Vol. 6002, Nanofabrication: Technologies, Devices, and Applications II, 60020N-1 (2005).

[13]K. Kohmura, H. Tanaka, S. Oike, M Murakami, T. Ono, Y. Seino, and T. Kikkawa, Mater. Res. Soc. Symp. Proc. **863**, B3.10.1 (2005).

[14]H. Miyoshi, H. Hatsuo, Y. Oku, H. Tanaka, K. Yamada, N. Mikami, S. Takada, N. Hata, and T. Kikkawa, Jpn. J. Appl. Phys. **43**, 498 (2004).

[15]H. Tada, K. Nakamura, and H. Nagayama, J. Phys. Chem. **98**, 12452 (1994).

[16]D. D. Burkey and K. K. Gleason, J. Appl. Phys. Vol. **93**, 5143 (2003).

[17]*Silicone Compounds Register and Review*, edited by B. Arkles (Petrarch Systems, Bristol, PA, 1987).

[18]K. Kohmura, H. Tanaka, S. Oike, M. Murakami, N. Fujii, S. Takada, T. Ono, Y. Seino, and T. Kikkawa, Thin Solid Films **515**, 5019 (2007).

[19]D. D. Burkey and K. K. Gleason, Mat. Res. Soc. Symp. Proc. **766**, E6.7.1 (2003).

[20]G. Lucovsky, J. Yang, S. S. Chao, J. E. Tyler, and W. Czubatyj, Phys. Rev. B **28**, 3225 (1983).

[21]M. J. Loboda, C. M. Grove, and R. F. Schneider, J. Electrochem. Soc. **145**, 2790 (1998).

[22]M. G. Albrecht and C. Blanchette, J. Electrochem. Soc. **145**, 4019 (1998).

[23]P. Bornhauser and G. Calzaferri, Spectrochim. Acta. Part A **46**, 1045 (1990).

[24]P. Bornhauser and G. Calzaferri, J. Phys. Chem. **100**, 2035 (1996).

[25]C. Marcolli and G. Calzaferri, J. Phys. Chem. **101**, 4925 (1997).

[26]M. Kuhn and D. J. Silversmith, J. Electrochem. Soc., **118**, 966 (1971).

[27]A. Mallikarjunan and S. P. Murarka, J. Appl. Phys. **95**, 1216 (2004).

[28]A. Mallikarjunan, S. P. Murarka, and T.-M. Lu, J. Electrochem. Soc. **149**, F155 (2002).

[29]A. Mallikarjunan, S. P. Murarka, and T.-M. Lu, Appl. Phys. Lett. **79**, 1855 (2001).

[30]N. Lifshitz, G. Smolinsky, and J. M. Andrews, J. Electrochem. Soc. **136**, 1440 (1989).

[31]N. Lifshitz and G. Smolinsky, J. Electrochem. Soc. **136**, 2335 (1989).

[32]Y. Abe, H. Hosono, W. H. Lee, and T. Kasuga, Phys. Rev. B **48**, 15 621 (1993).

[33]C. Fritzsche, Z. *angew-Phys*. **24**, 48 (1967).

[34]Y. S. Li and P. M. Duxbury: Phys. Rev. B **40**, 4889 (1989).

Figure captions

FIG. 1. Cs/Si atomic ratio from Rutherford backscattering spectrometry (RBS) as a function of Cs density (a). O/Si atomic ratio from RBS (b).

FIG. 2. Elastic modulus from nano indentation as a function of porosity. M_w means the elastic modulus of silica skeleton determined by using eq.(2). The porosity was calculated from the dielectric constant with Rayleigh equation of eq.(1).

FIG. 3. Pore size distribution of porous silica measured from positron annihilation lifetime spectroscopy (PALS).

FIG. 4. Fourier transform infrared spectra (FTIR) of porous silica film at higher wave numbers (a) and the spectra at lower wave numbers (b). Adsorption intensity was normalized to film thickness and pore surface area. Each peak assignment is described in text.

FIG. 5. Each peak area of FT-IR spectrum due to O-H stretching mode of silanol group (a), C-H stretching mode of methyl group (b), H-Si stretching mode of D-type structure ($HSiO_2(CH_3)$) and H-Si T-type structure ($HSiO_3$) of polymerized TMCTS (c), and area ratio of D-type to CH_3 and H-S T-type to D-type (d). The connecting line is merely guide for eye.

FIG. 6. Dielectric constant (k) calculated from capacitance of Au/PoSiO/Si structure as a function of relative humidity condition (R_h).

FIG. 7. Number density of adsorbed water (N) as a function of relative humidity (R_h) at room temperature of 20°C, which was derived from the dielectric constant and relative humidity relation (Fig. 6) (a). A Brunauer-Emmett-Teller (BET) plot of the water adsorption isotherm (b).

FIG 8. Number density of water adsorption site (N_m) as a function of doped Cs concentration (a). A

relation between N_m and total O-H area (S_{OH}) in FT-IR spectra (b).

FIG. 9. Leakage current density with $/E/ = 1$ MV/cm as a function of time. Under N_2 ambient at 20°C or 200°C (a). Under humid vapor of RH 59% at 20°C (b).

FIG. 10. Leakage current density (J) - electric field strength (E) property for Cs 0, 5, 15, 30 ppm PoSiO, respectively. Relative humidity condition (RH) was changed from 2% to 65%.

FIG. 11. Leakage current density (J) - electric field strength (E) property at 200°C after a constant stress $/E_c/ = 1$ MV/cm was applied. The result of Cs 0 ppm porous silica (a). The ramp rate (β) of E was changed as 0.1, 0.2, 1 V/sec. The results of Cs 0, 5, 15, 30 ppm porous silica (b).

FIG. 12. Leakage current density (J) - electric field strength (E) property at 200°C under N_2 ambient for Cs 0, 5, 15, 30 ppm porous silica. Solid line means a permanent dielectric breakdown mode. Dashed line means an instantaneous dielectric breakdown mode.

FIG. 13. Weibull distribution of time zero dielectric breakdown field strength (E_{DB}) for Cs 0, 5, 15, 30 ppm porous silica. Connecting lines are merely guide for eye.

FIG. 14. Time dependent dielectric breakdown lifetime of 50% probability under N_2 ambient. The results at 200°C for Cs 0, 5, 15, 30 ppm porous silica (a). The dashed line represents the fitting line with eq.(5) for Cs 15 ppm porous silica. The solid line represents the fitting line for Cs 30 ppm. The dotted lines for Cs 0 and 5 ppm PoSiO are guide for eye. The results for Cs 30 ppm porous silica (b). Substrate temperature was changed as 180°C, 200°C, and 220°C.
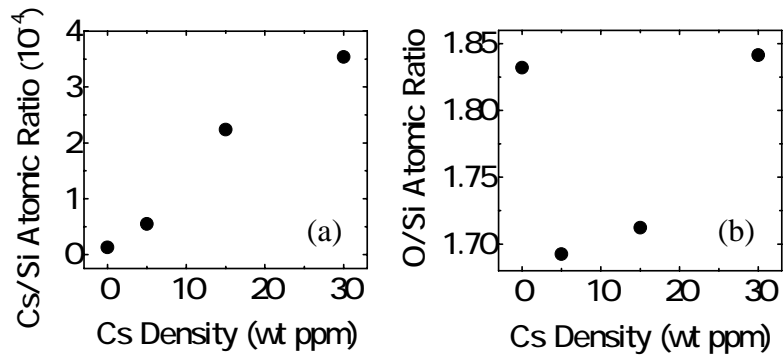
Figure 1. Y. Kayaba et al, Journal of Electrochemical Society.
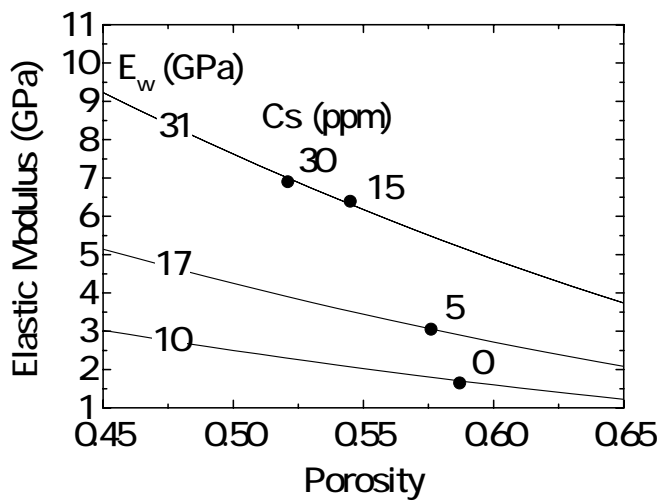
Figure 2. Y. Kayaba et al, Journal of Electrochemical Society.
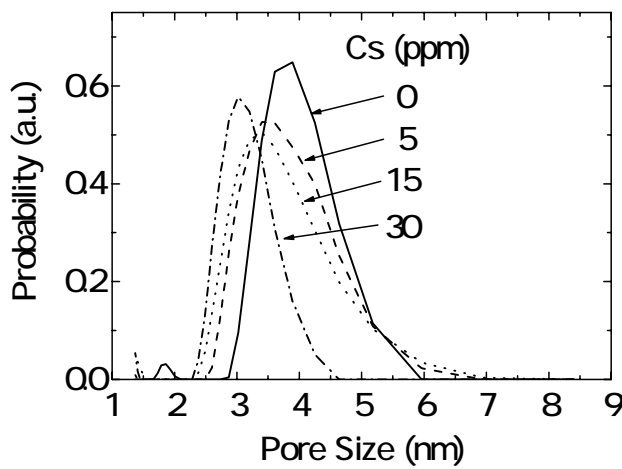
Figure 3. Y. Kayaba et al, Journal of Electrochemical Society.
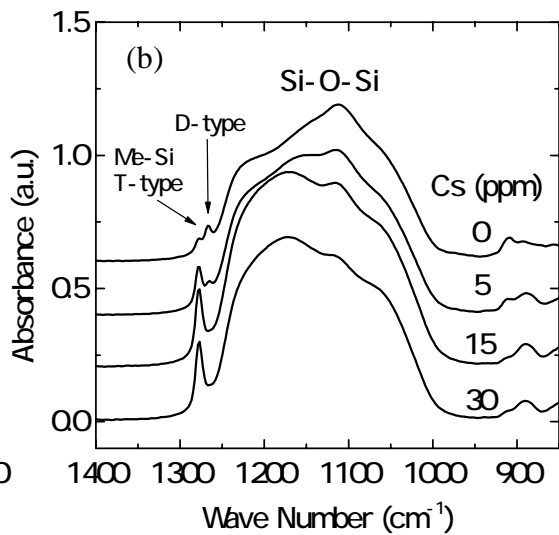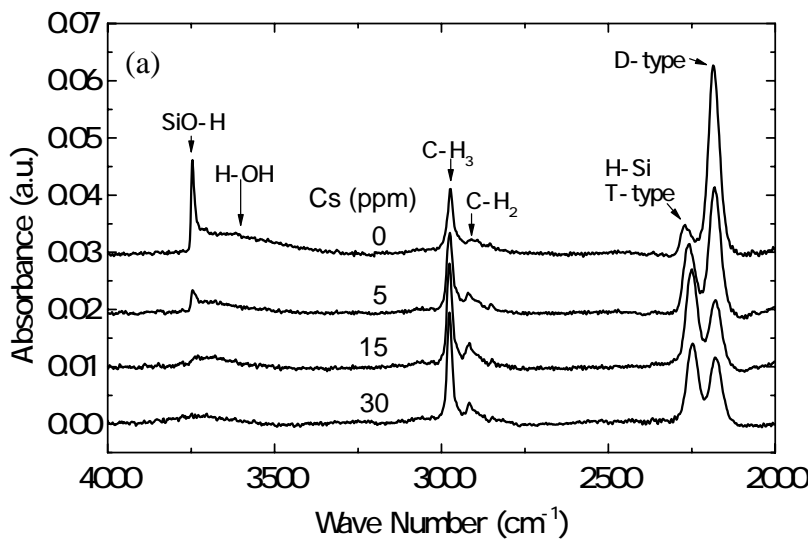
Figure 4. Y. Kayaba et al, Journal of Electrochemical Society.
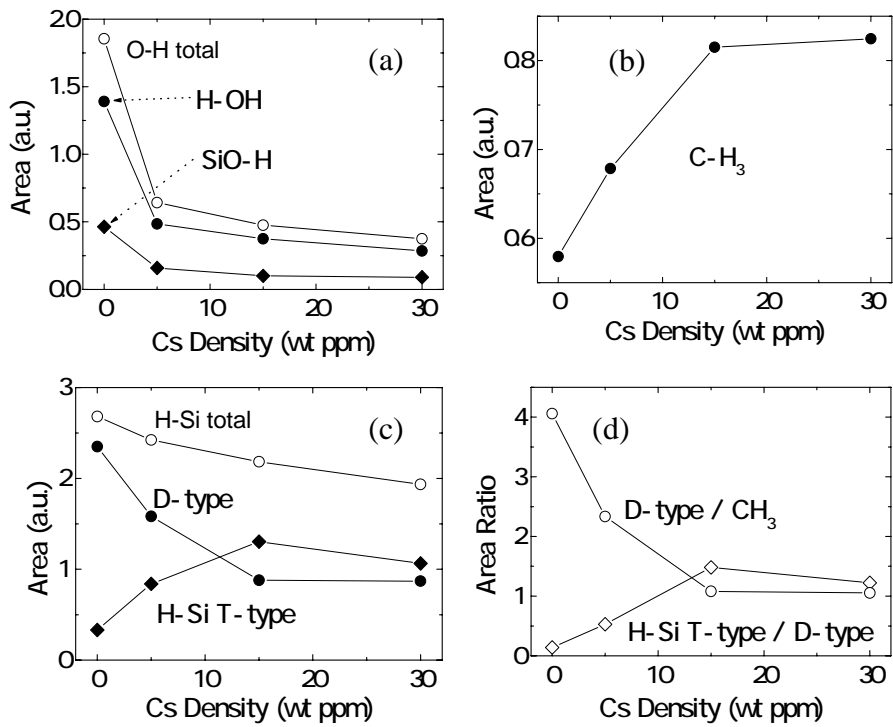
Figure 5. Y. Kayaba et al, Journal of Electrochemical Society.
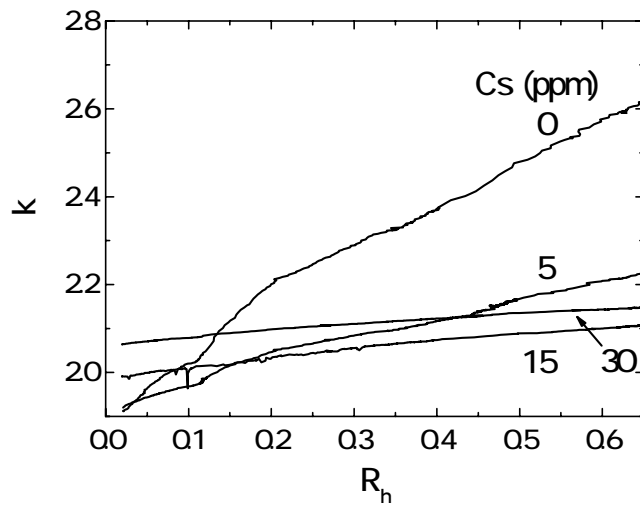
Figure 6. Y. Kayaba et al, Journal of Electrochemical Society.
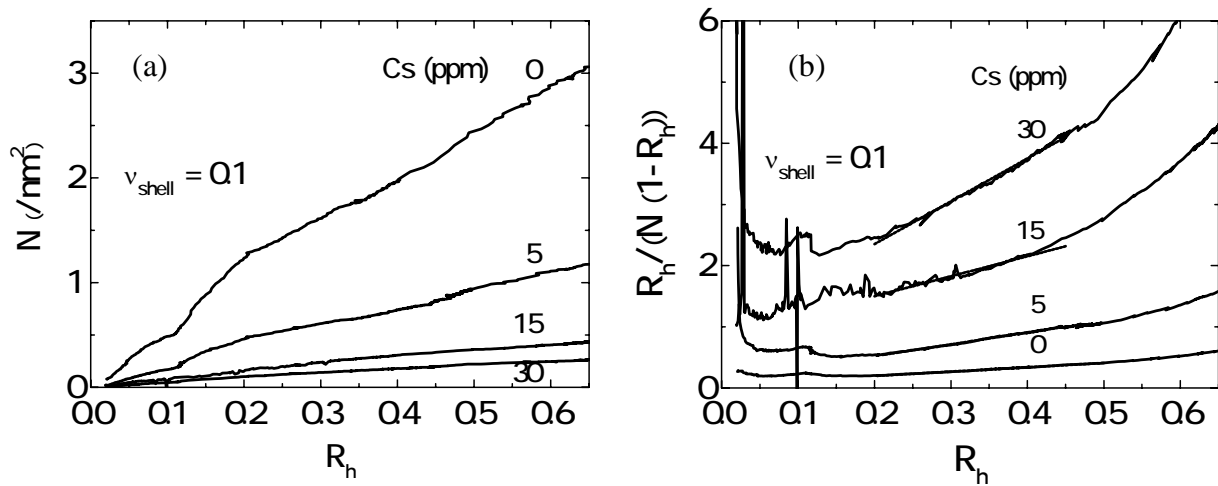
Figure 7. Y. Kayaba et al, Journal of Electrochemical Society.

(a)

N_m (/nm^2)

Cs Density (wt ppm)

(b)

N_m (/nm^2)

S_{OH} (a.u.)

$N_m = A + B \, S_{OH}$

$A = -0.1057 \pm 0.068$

$B = 0.772 \pm 0.066$
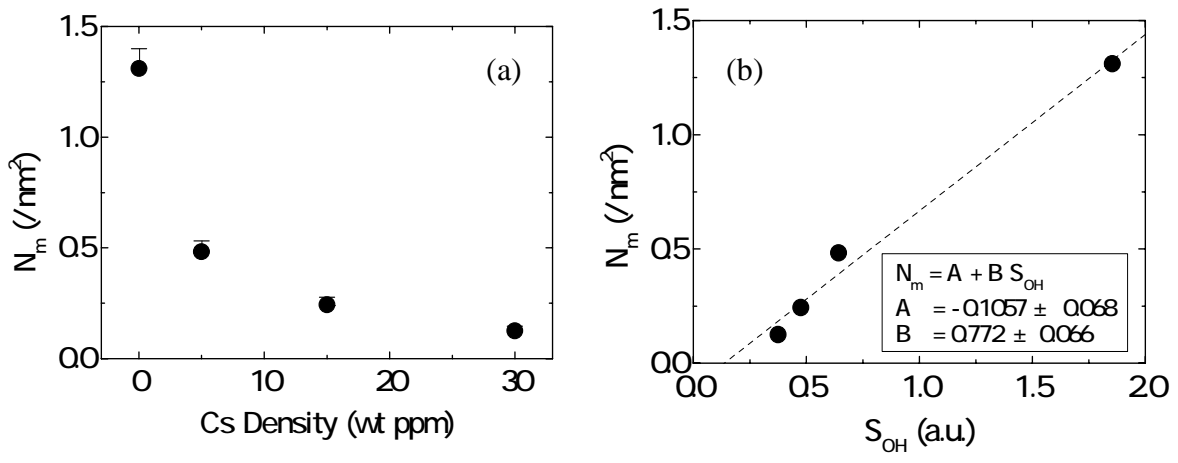
Figure 8. Y. Kayaba et al, Journal of Electrochemical Society.
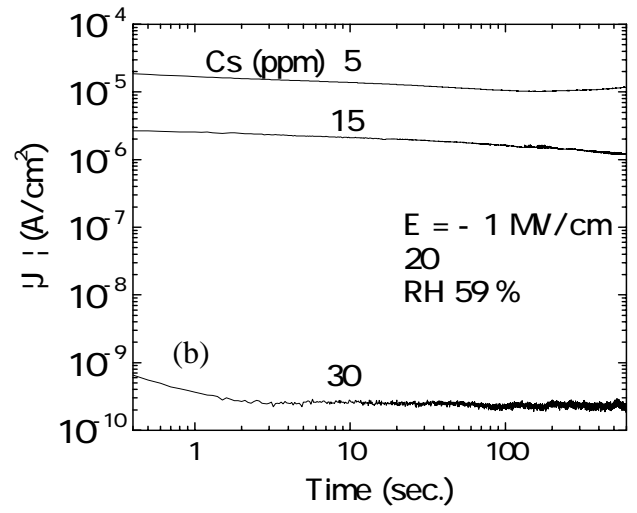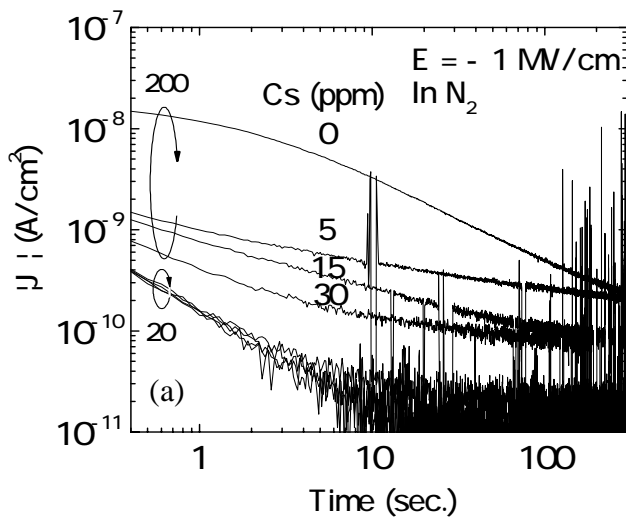
Figure 9. Y. Kayaba et al, Journal of Electrochemical Society.
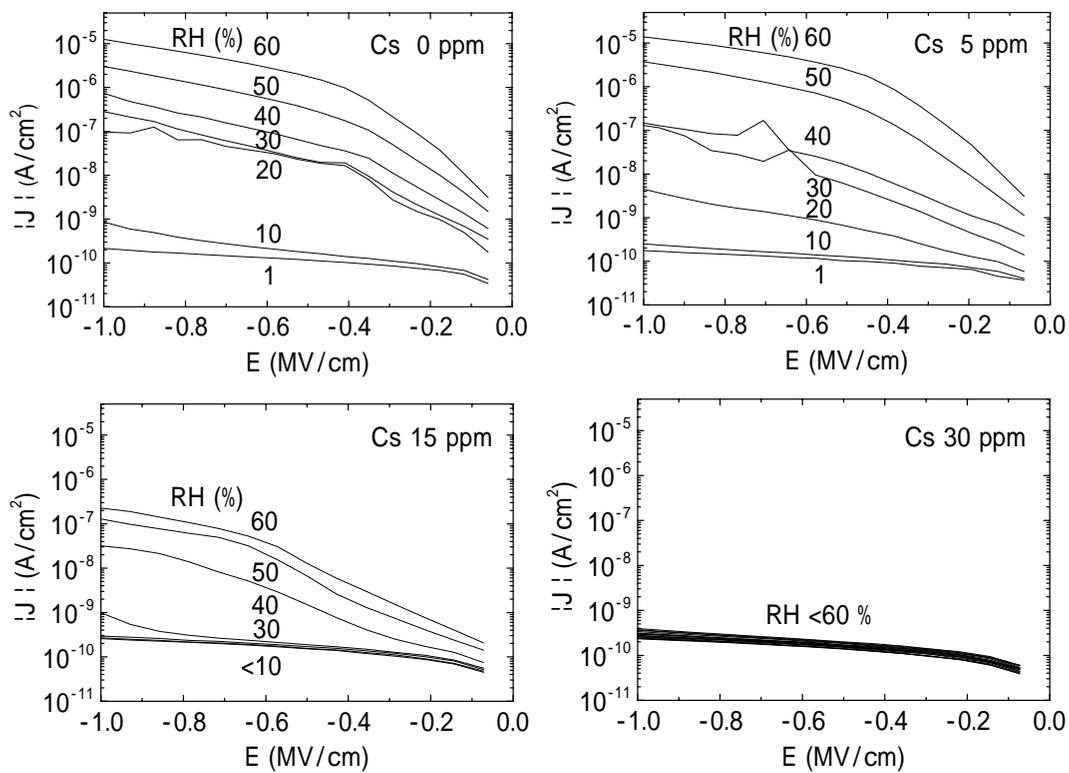
Figure 10. Y. Kayaba et al, Journal of Electrochemical Society.
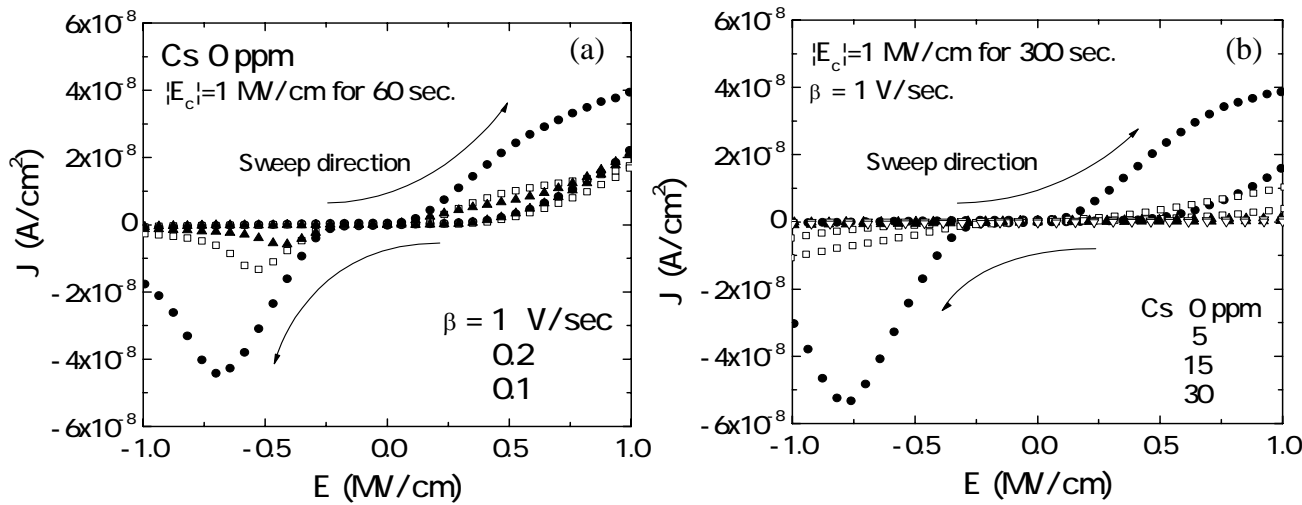
Figure 11. Y. Kayaba et al, Journal of Electrochemical Society.
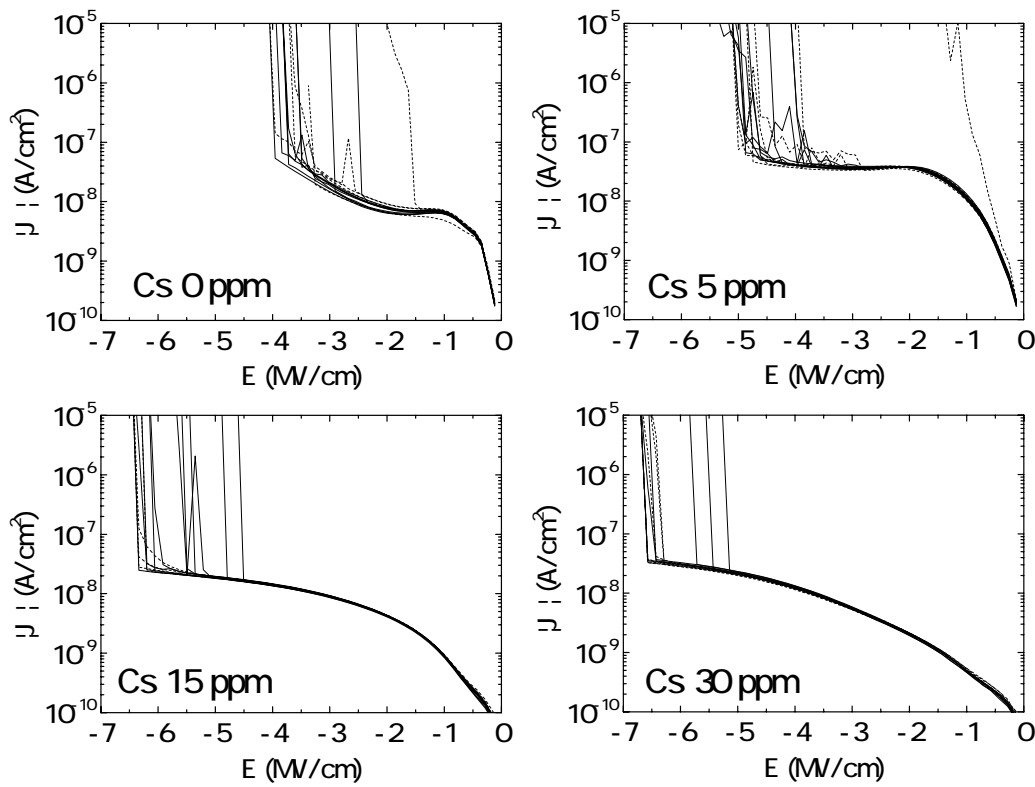
Figure 12. Y. Kayaba et al, Journal of Electrochemical Society.
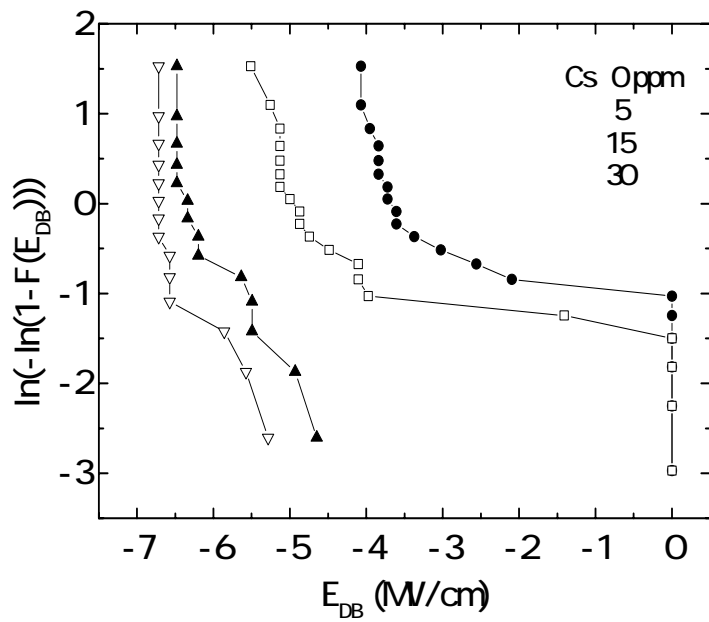
Figure 13. Y. Kayaba et al, Journal of Electrochemical Society.
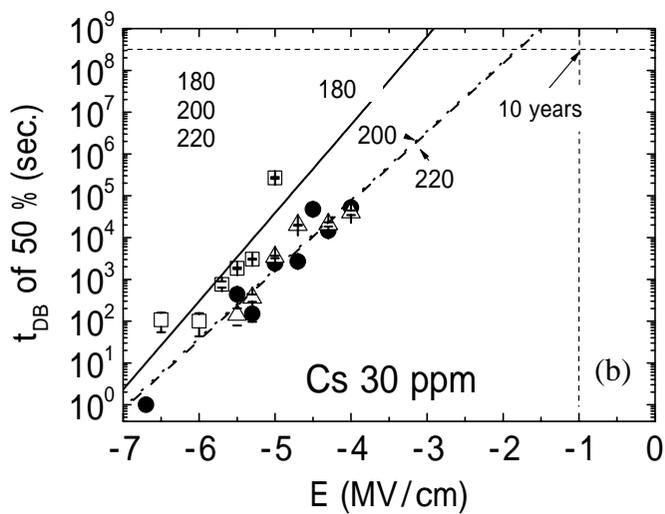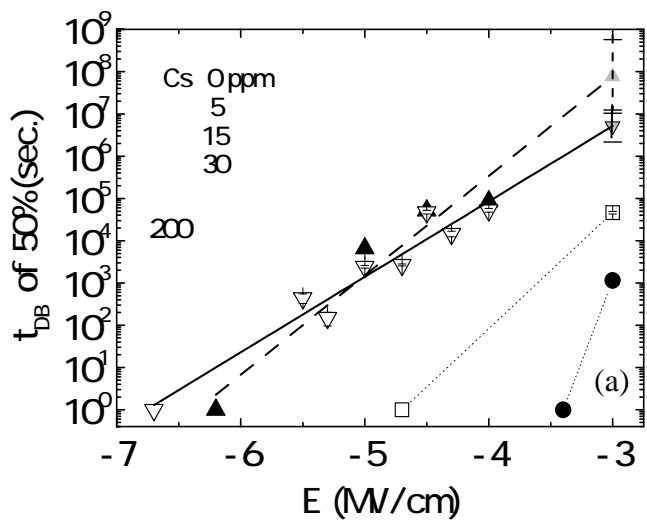
Figure 14. Y. Kayaba et al, Journal of Electrochemical Society.